

Supporting Information

Electrocatalytic and Conductive Vanadium Oxide on Carbonized Bacterial Cellulose Aerogel for the Sulfur Cathode in Li-S Batteries

Xueyan Lin¹, Wenyue Li², Xuan Pan³, Shu Wang⁴ and Zhaoyang Fan^{2,*}

¹School for Engineering of Matter, Transport & Energy, Arizona State University, Tempe, Arizona, 85281, USA

²School of Electrical, Computer and Energy Engineering, Arizona State University, Tempe, AZ 85281, USA

³Institutes of Science and Development, Chinese Academy of Sciences, Beijing 100190, China

⁴College of Health Solutions, Arizona State University, Phoenix, Arizona, 85004, USA

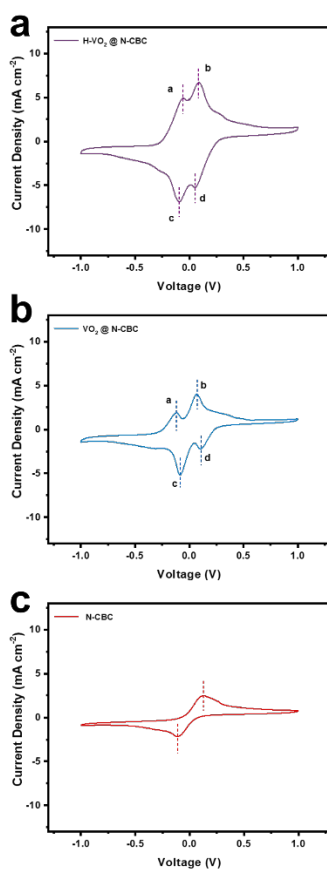


Figure S1 The CV curves of H-VO₂@N-CBC, VO₂@N-CBC, and N-CBC -based electrodes in a symmetric cell with Li₂S₆ as the electrolyte at the scan rate of 3 mV/s. The redox peaks are labeled as a, b, c, and d, respectively.

Supplementary Note S1. The details on calculation of activation energy change.

CV tests were performed under a scan rate of 0.2 mV/s at 298 K as shown in Fig 3a. The relationship between the electrode potential and the activation energy is given by the equation (eq. 1) [1,2]:

$$E_a = E_a^0 + \alpha z F \varphi_{(Red)ir}$$

where E_a is the activation energy of reduction process, E_a^0 is the intrinsic activation energy, α is the symmetry factor, z is the charge transfer number, F is the Faraday's constant, $\varphi_{(Red)ir}$ is the irreversible potential during the reduction process, which can be read from the peak potential in CV curves during the reduction process.

The Tafel equation (eq. 2):

$$\eta = \frac{RT}{\alpha z F} \ln j_0 - \frac{RT}{\alpha z F} \ln j$$

Where η is the overpotential, R is the gas constant, T is the absolute temperature, j_0 is the exchange current density, j is the current density. The equation can be simplified in a concise form (eq. 3):

$$\eta = a + b \ln j$$

Therefore, a is the intercept of Tafel curve (eq. 4):

$$a = \frac{RT}{\alpha z F} \ln j_0$$

and b is the slope of Tafel curve (eq. 5):

$$b = -\frac{RT}{\alpha z F}$$

By substituting Tafel slope (eq. 5) into (eq. 1), we can rewrite a concise form:

$$E_a = E_a^0 - \frac{RT}{b} \varphi_{(Red)ir}$$

Consequently, based on the Tafel slope as shown in Fig. 3 (e and f), the activation energy during discharge (reduction) process can be calculated.

The activation energy corresponds to the reduction from S_8 to Li_2S_n :

$$\text{N-CBC based electrode: } E_{a1} = E_{a1}^0 - 73.79 \text{ kJ mol}^{-1}$$

$$\text{VO}_2@\text{N-CBC based electrode: } E_{a1}' = E_{a1}^0 - 90.24 \text{ kJ mol}^{-1}$$

$$\text{H-VO}_2@\text{N-CBC based electrode: } E_{a1}'' = E_{a1}^0 - 101.97 \text{ kJ mol}^{-1}$$

The difference in activation energy can be calculated by subtracting the activation energy between two different electrodes:

Activation energy difference between $\text{VO}_2@\text{N-CBC}$ and N-CBC based electrodes:

$$E_{a1} - E_{a1}' = (E_{a1}^0 - 73.79) \text{ kJ mol}^{-1} - (E_{a1}^0 - 90.24) \text{ kJ mol}^{-1} = 16.45 \text{ kJ mol}^{-1}$$

Activation energy difference between H-VO₂@N-CBC and VO₂@N-CBC based electrodes:

$$E_{a1}' - E_{a1}'' = (E_{a1}^0 - 90.24) \text{ kJ mol}^{-1} - (E_{a1}^0 - 101.97) \text{ kJ mol}^{-1} = 11.73 \text{ kJ mol}^{-1}$$

Similarly, we can calculate the relative activation energy among three electrodes from Li₂S_n to Li₂S.

Table S1. Comparison of the electrochemical performance of LSBs using different catalytic materials.

Catalytic materials	Sulfur loading (mg/cm ²)	Rate capability (mAh/g)	Cycling performance (mAh/g)	Ref.
VO ₂ (R)/V ₂ O ₃	2.5	957/1C	758/300th (1C)	This work
VN	1.3–1.5	850/2C	~750/500th(0.5C)	[3]
VO ₂ (P)	2.0	760/2C	780/500th(2C)	[4]
VO ₂ (B)	1.4–2.0	831/2C	615/200th(2C)	[5]
Ti ₄ O ₇	1.5–1.8	850/2C	~940/100th (0.5C)	[6]
MnO ₂	0.7–1.0	950/1C	1030/200th (0.2C)	[7]
TiO ₂ -TiN	1.0–1.2	682/2C	927/300th (0.3C)	[6]
RuO ₂	1.5	543/2C	508/200th (1C)	[8]

1. Hua, W.; Li, H.; Pei, C.; Xia, J.; Sun, Y.; Zhang, C.; Lv, W.; Tao, Y.; Jiao, Y.; Zhang, B.; et al. Selective Catalysis Remedies Polysulfide Shuttling in Lithium-Sulfur Batteries. **2021**, 33, 2101006, doi:<https://doi.org/10.1002/adma.202101006>.
2. Cho, J.; Ryu, S.; Gong, Y.J.; Pyo, S.; Yun, H.; Kim, H.; Lee, J.; Yoo, J.; Kim, Y.S. Nitrogen-doped MoS₂ as a catalytic sulfur host for lithium-sulfur batteries. *Chemical Engineering Journal* **2022**, 439, 135568, doi:<https://doi.org/10.1016/j.cej.2022.135568>.
3. Li, F.; Zhang, M.; Chen, W.; Cai, X.; Rao, H.; Chang, J.; Fang, Y.; Zhong, X.; Yang, Y.; Yang, Z.; et al. Vanadium Nitride Quantum Dots/Holey Graphene Matrix Boosting Adsorption and Conversion Reaction Kinetics for High-Performance Lithium–Sulfur Batteries. *ACS Applied Materials & Interfaces* **2021**, 13, 30746-30755, doi:10.1021/acsami.1c08113.
4. Wang, S.; Liao, J.; Yang, X.; Liang, J.; Sun, Q.; Liang, J.; Zhao, F.; Koo, A.; Kong, F.; Yao, Y.; et al. Designing a highly efficient polysulfide conversion catalyst with paramontroseite for high-performance and long-life lithium-sulfur batteries. *Nano Energy* **2019**, 57, 230-240, doi:<https://doi.org/10.1016/j.nanoen.2018.12.020>.
5. Song, Y.; Zhao, W.; Zhu, X.; Zhang, L.; Li, Q.; Ding, F.; Liu, Z.; Sun, J. Vanadium Dioxide-Graphene Composite with Ultrafast Anchoring Behavior of Polysulfides for Lithium–Sulfur Batteries. *ACS Applied Materials & Interfaces* **2018**, 10, 15733-15741, doi:10.1021/acsami.8b02920.
6. Zhou, T.; Lv, W.; Li, J.; Zhou, G.; Zhao, Y.; Fan, S.; Liu, B.; Li, B.; Kang, F.; Yang, Q.-H. Twinborn TiO₂-TiN heterostructures enabling smooth trapping–diffusion–conversion of polysulfides towards ultralong life lithium–sulfur batteries. *Energy & Environmental Science* **2017**, 10, 1694-1703, doi:10.1039/C7EE01430A.
7. Liang, X.; Hart, C.; Pang, Q.; Garsuch, A.; Weiss, T.; Nazar, L.F. A highly efficient polysulfide mediator for lithium–sulfur batteries. *Nature Communications* **2015**, 6, 5682, doi:10.1038/ncomms6682.

8. Huang, J.-Q.; Huang, J.; Chong, W.G.; Cui, J.; Yao, S.; Huang, B.; Kim, J.-K. Graphene/RuO₂ nanocrystal composites as sulfur host for lithium-sulfur batteries. *Journal of Energy Chemistry* **2019**, 35, 204-211, doi:<https://doi.org/10.1016/j.jechem.2019.03.017>.